Coexistence of bound and localized exciton magnetic polarons in $Cd_{0.8}Mn_{0.2}Te$

2007 J. Phys.: Condens. Matter 19 186210

(http://iopscience.iop.org/0953-8984/19/18/186210)

IOP PUBLISHING JOURNAL OF PHYSICS: CONDENSED MATTER

J. Phys.: Condens. Matter **19** (2007) 186210 (10pp) doi:10.1088/0953-8984/19/18/186210

Coexistence of bound and localized exciton magnetic polarons in $Cd_{0.8}Mn_{0.2}Te$

Takanori Okada[1,2] **and Tadashi Itoh**[2]

[1] Pioneering Research Unit for Next Generation, Kyoto University, Kyoto 615-8245, Japan
[2] Division of Materials Physics, Graduate School of Engineering Science, Osaka University, Osaka 560-8531, Japan

Received 24 November 2006, in final form 2 March 2007
Published 5 April 2007
Online at stacks.iop.org/JPhysCM/19/186210

Abstract

Fundamental magneto-optical properties of single crystals of the semimagnetic semiconductor $Cd_{0.8}Mn_{0.2}Te$ are carefully measured with the use of band-to-band excitation. Two new phenomena are presented: the peculiar magnetic field dependence of the magnetic polaron luminescence and the existence of two components for the polaron luminescence. Theoretical consideration with regard to the Zeeman effect ascribes the two components of luminescence to the exciton magnetic polaron spectrum and the neutral acceptor-bound exciton magnetic polaron spectrum. The calculated result for the luminescence peak positions is also consistent with the experimental result of the circularly polarized luminescence under the presence of an applied magnetic field. In other words, the σ^+ luminescence is due to the exciton magnetic polaron, whereas the σ^- luminescence is due to the neutral acceptor-bound exciton magnetic polaron.

1. Introduction

A II–VI semimagnetic semiconductor (SMSC) that includes $Cd_{1-x}Mn_xTe$, also called a II–VI diluted magnetic semiconductor, is a paramagnetic compound semiconductor with the addition of magnetic ions. The optical properties of this material have been studied for over 20 years and the systematic understanding is well established [1]. The physical properties of $Cd_{1-x}Mn_xTe$ are characterized by the usual semiconductor mixed-crystal effects as well as by the special magnetic properties caused by the half-filled 3d-shell of Mn^{2+} cations. According to virtual crystal approximation, the alloy potential should fluctuate, which is essential since it leads to the intrinsic localization of the photoexcited excitons in these mixed compounds. The most important physical properties are based on the strong sp–d exchange interaction between the 5s-electron or 5p-hole band states and the Mn^{2+} 3d-electron states. Due to this exchange interaction, the effective g-factor of $Cd_{1-x}Mn_xTe$ can be enhanced by up to two orders of

magnitude larger than that of CdTe. This exchange interaction then leads to peculiar magneto-optical effects such as the giant Zeeman splitting of the valence and conduction bands [2], giant Faraday rotation [3], photo-induced magnetization [4], and the formation of a magnetic polaron (MP) [5]. Usually, the II–VI SMSCs are suitable materials with controllable parameters to use for studying the various mechanisms responsible for both magnetic and semiconducting properties. Due to the discovery of ferromagnetism, the III–V SMSCs have recently proven very useful for building a semiconductor device for spintronics, such as the injection of spin-polarized electrons into a non-magnetic semiconductor [6] or a light-emitting diode [7].

Among the properties mentioned above, one outstanding problem is the photo-induced magnetic-phase transition in paramagnetic SMSCs. The localization of the excitons should induce the alignment of the magnetic spins inside the exciton's Bohr radius, thereby resulting in the formation of an exciton magnetic polaron (EMP) bound to an alloy potential fluctuation (APF) or an impurity. Due to this mechanism, it is generally predicted that the ferromagnetic region will be induced into the paramagnetic system by photo-excitation. However, this phase transition has not yet been realized by optical pumping. Therefore, it is important to understand fully the exciton localization and its luminescence in these materials. The photoluminescence lines of SMSCs show some characteristic behaviour. The asymmetric or inhomogeneous photoluminescence in $Cd_{1-x}Mn_xTe$ at various temperatures and magnetic fields has been reported [8]. It has been theorized that the inhomogeneous linewidth of this photoluminescence arises from the exciton localization by pinning to the defect centre with random configurations and by APF. Therefore, the shape of the photoluminescence spectrum is a symmetric Gaussian when the exciton is localized through the hole, i.e. the MP effect. Alternatively, APF causing a one-particle exciton localization results in an asymmetric Gaussian profile. In our previous paper [9], this characteristic behaviour of the photoluminescence lines in $Cd_{0.8}Mn_{0.2}Te$ was reported at various temperatures, magnetic field strengths, and excitation energies. From the line-shape analysis, the photoluminescence spectra have been examined qualitatively and consist of two components attributed to the EMP (called $L2$) and the neutral acceptor-bound magnetic polaron (A^0XBMP) (called $L1$). Each component is asymmetric due to the APF effect.

In this paper, the observed double peaks of luminescence are discussed quantitatively considering giant Zeeman effects. A consistent explanation is given for the new spin-related optical phenomena and this may be useful for the consideration of the photo-induced magnetic phase transition. The photoluminescence was studied through various optical measurements, e.g. the dependencies of time, magnetic field strength, and circular polarization. A single crystal of $Cd_{0.8}Mn_{0.2}Te$ in which the localization energies due to the magnetic polaron formation would be larger than that due to APF [10] is essential for the observation of the double peaks. Above this concentration of Mn^{2+}, the behaviour of photoluminescence becomes more complicated due to the appearance of a spin-glass phase at low temperatures [11].

2. Experiment

Single crystals of $Cd_{0.8}Mn_{0.2}Te$ were grown using the Bridgman method. The plank-shaped samples were obtained by cleaving the middle of a cylindrical $Cd_{0.8}Mn_{0.2}Te$ ingot perpendicular to its axis. For the band-to-band excitation the second harmonic of an Nd:YVO_4 laser (2.37 eV) was used as an excitation source. In the case of measurement with a circularly polarized excitation source, a linear polarizer and a quarter-wave plate were placed in front of the sample. The excitation light was incident perpendicular to the surface of the sample. The area of the excitation spot on the sample was 0.5 mm^2. The excitation power was reduced sufficiently to avoid any heating of the sample. A magnetic field of up to 7 T was applied

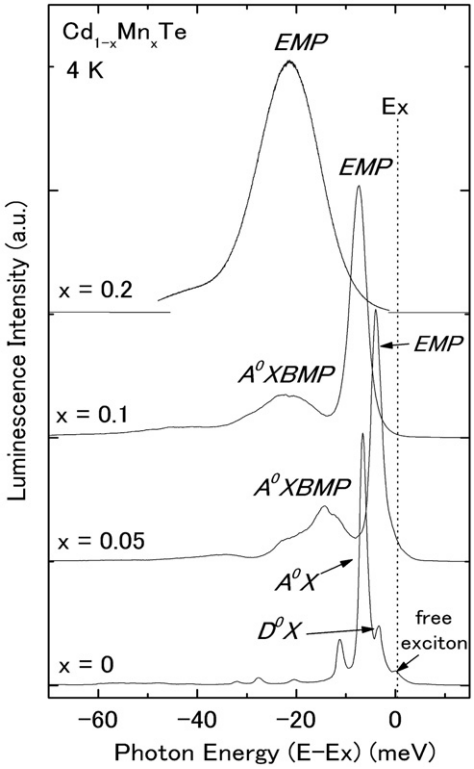

Figure 1. Stationary photoluminescence spectra of excitons in $Cd_{1-x}Mn_xTe$ without a magnetic field at various Mn compositions. The peak intensity is normalized with the dominant peak intensity. E_x is the free exciton energy determined from the exciton-reflection spectrum. The description of A^0X and D^0X are explained in the text.

in the Faraday configuration. The temperature of the sample was controlled in the cryostat with a continuous flow of liquid helium and a heater. The backward photoluminescence from the sample was passed through a quarter-wave plate and a polarizer to separate the σ^+ and σ^- circularly polarized components. The photoluminescence, which first passed through a spectrometer, was detected by a cooled charge-coupled device. The spectral resolution was 0.3 meV. In the case of the time-resolved experiment, the second harmonic light of the 76 MHz mode-locked Ti–sapphire laser generated by $LiNbO_3$ was used as the picosecond light source at 800 nm (1.55 eV). For a detector, a streak camera working in the synchroscan mode was used. The overall time resolution was approximately 10 ps.

3. Results and discussion

Figure 1 shows the profiles of the stationary photoluminescence spectra of free and bound excitons, EMP ($L2$), and A^0XBMP ($L1$) under band-to-band excitation in $Cd_{1-x}Mn_xTe$ without the application of a magnetic field at various Mn compositions. The peak intensity is normalized with the dominant peak intensity. E_x is the free exciton energy determined from the exciton-reflection spectrum. In the case of $x = 0$, namely CdTe, three photoluminescence lines representing an exciton bound to a neutral acceptor (A^0X), an exciton bound to a neutral donor (D^0X) and a free exciton are observed. In the case of mixed crystals with Mn^{2+} ions, the

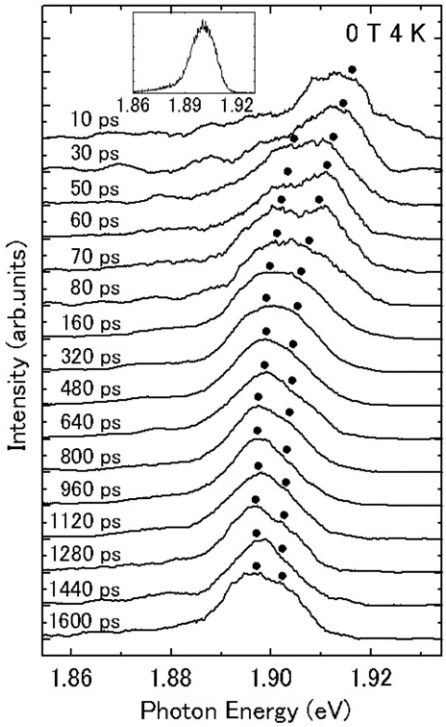

Figure 2. Time evolution of the photoluminescence spectrum in $Cd_{0.8}Mn_{0.2}Te$ in the absence of a magnetic field. The peak intensity is normalized. In the first 100 ps, the shift of the lines is attributed to exciton localization and MP formation. The closed circles represent the peak positions only as guides for the eyes. The inset shows the integrated photoluminescence spectrum.

photoluminescence is dominated by two features, $L1$ and $L2$, at Mn compositions of x smaller than 0.1, whereas the compositions of $x = 0.2$ show only a single peak.

In the time evolution of the photoluminescence spectra in $Cd_{0.8}Mn_{0.2}Te$, the photoluminescence demonstrates an irregular behaviour, as shown in figure 2. As shown by the closed circles, a doublet peak structure can be observed over different time intervals. Therefore, the photoluminescence of $Cd_{0.8}Mn_{0.2}Te$ may consists of two components. To clarify the origin of these doublet peaks, the circular polarization dependence of the photoluminescence with magnetic field strength was measured. In the Faraday configuration, there are two magnetic subcomponents with the σ^+ and the σ^- circular polarizations. For the free exciton transition, only the σ^+ photoluminescence should appear, because this transition originates from the lowest energy level of the exciton in thermal equilibrium. However, in this experiment, not only σ^+ but also σ^- photoluminescence is observed under band-to-band excitation, as shown in figure 3. Each polarized component is completely separated, because the peak positions are obviously observed at different positions, as shown in the inset of figure 3. The magnetic field dependences of the energy positions of the σ^+ luminescence peaks ($\bigtriangledown$), the σ^- luminescence peaks ($\bigcirc$), and the reflectivities ($\diamond$) are shown in figure 4. A similar phenomenon, or the appearance of the σ^- luminescence at the lower energy side of the σ^+ luminescence, was observed for $Cd_{0.88}Mn_{0.12}Te$, but explained merely qualitatively with regard to light and heavy holes [12]. Therefore, a quantitative interpretation of the σ^+ and σ^- components is given along with a qualitative explanation for their peak energy positions from the standpoint of the polarization and the external magnetic field strength.

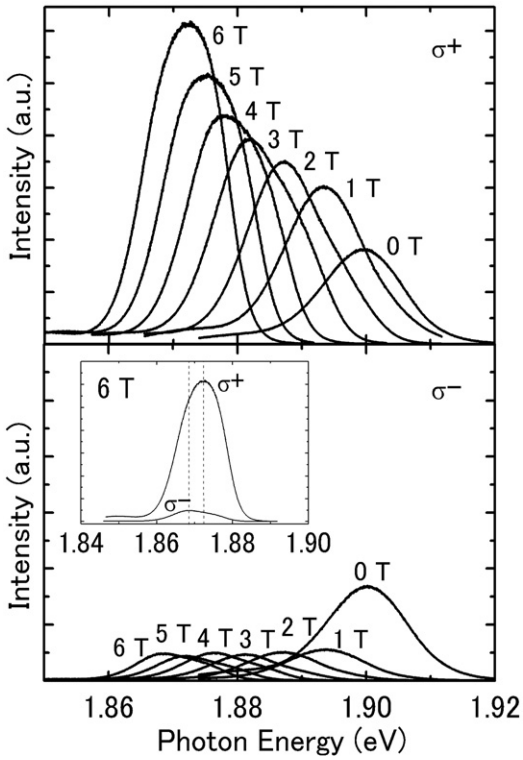

Figure 3. Photoluminescence evolution as a function of magnetic field strength for σ^+ components (top) and for σ^- components (bottom). The inset shows a comparison of the σ^- and σ^+ line-shapes at 6 T. The intensity of the σ^+ photoluminescence at 0 T is the same as that of the σ^- one.

At $T = 4$ K, the energy positions for the $L1$ (EMP) and $L2$ (A^0XBMP) peaks are reported as follow [13]:

$$E_{L1} = 1588.8 + 1440x \text{ meV} \qquad (0 < x \leqslant 0.1) \tag{1}$$

$$E_{L2} = 1604.7 + 1397x \qquad (0.05 \leqslant x \leqslant 0.2) \tag{2}$$

$$= 1575.0 + 1536x \qquad (0.2 \leqslant x \leqslant 0.4). \tag{3}$$

Each photoluminescence band has a broad width due to the APF and MP effects. As for the $L1$ line, the energy position is difficult to determine for $x > 0.1$ because of the overlap of the $L1$ and $L2$ lines, although the $L1$ line is observable up to $x = 0.2$ [14]. When equation (1) is extrapolated to the Mn concentration of $x = 0.2$ and compared with equations (2) and (3), these energy values are found to be coincident with the peak positions obtained experimentally. Therefore, the high- and low- energy peaks are postulated to be the $L2$ and $L1$ lines, respectively.

In order to clarify quantitatively that the $L2$ and $L1$ lines are attributed to the σ^+ and σ^- photoluminescences, respectively, a comparison between the experimental and theoretical results is necessary. First, we consider the $L2$ line. The transition energy E_{tran} between the valence band and the conduction band can be calculated by taking into account the sp–d exchange interaction between the spins of the band electron (5s or 5p orbit) and the Mn^{2+} spins (3d orbit) [15–17]. Usually, this exchange interaction is described phenomenologically

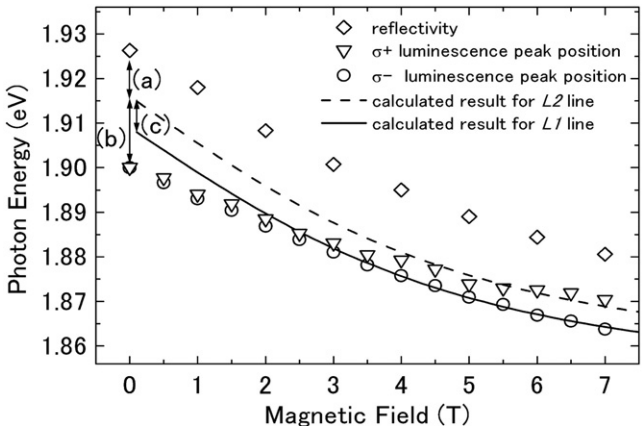

Figure 4. A comparison of the experimental photoluminescence peak positions with the calculated positions as functions of the magnetic field strength at 4 K. Because the MP and APF effect are not considered in the calculation, the calculated position departs from the photoluminescence peaks at low magnetic field strengths. The values of the localization energy due to the APF and the MP formation are determined to be (a) 11 meV and (b) 15 meV, respectively. The binding energy of the A^0X without the MP localization is assumed to be (c) 7 meV.

by a Heisenberg-type Hamiltonian as

$$H_{\mathrm{sp-d}} = \sum_{\vec{R}_i} J^{\mathrm{sp-d}}(\vec{r} - \vec{R}_i)\vec{S}_i \cdot \vec{\sigma}, \tag{4}$$

where $\vec{S}_i$ and $\vec{\sigma}$ are the spin operators of the Mn^{2+} ion on the lattice site $\vec{R}_i$ and of the band electron at $\vec{r}$, respectively. The term $J^{\mathrm{sp-d}}$ is the electron–ion sp–d exchange interaction energy, and the summation is over all Mn^{2+} ions. Applying the usual mean-field approximation and virtual-crystal approximation to equation (4), the transition energy is expressed as $E_g \pm \frac{1}{2}N_0(\alpha-\beta)x\langle S_z\rangle$ for the $|\pm\frac{1}{2}\rangle \rightarrow |\pm\frac{3}{2}\rangle$ transition and $E_g \mp \frac{1}{2}N_0(\alpha+\frac{1}{3}\beta)x\langle S_z\rangle$ for the $|\mp\frac{1}{2}\rangle \rightarrow |\pm\frac{1}{2}\rangle$ transition, where E_g is the energy of the forbidden gap in the absence of a magnetic field; $N_0\alpha$ and $N_0\beta$ are the exchange integrals of the s and p bands, respectively; x is the Mn^{2+} ion composition; and $\langle S_z\rangle$ is the average thermal value of $\vec{S}_i$. The notation $|m_s\rangle \rightarrow |m_j\rangle$ denotes the transition from the $|m_s\rangle$ electronic state in the conduction band to the $|m_j\rangle$ electronic state of the valence band. For the exciton of $Cd_{1-x}Mn_xTe$, the values $N_0\alpha$ and $N_0\beta$ are $+0.22$ eV and -0.88 eV, respectively. The average value $\langle S_z\rangle$ is written as

$$\langle S_z\rangle = -S_{\mathrm{eff}} B_{\frac{5}{2}}\left(\frac{5}{2}\frac{g_{\mathrm{Mn}}\mu_B B}{k_{\mathrm{B}}(T+T_0)}\right), \tag{5}$$

where $B_{\frac{5}{2}}$ is the Brillouin function for spin $S = \frac{5}{2}$, g_{Mn} is the g-factor of Mn^{2+}, μ_B is the Bohr magneton, k_{B} is the Boltzmann constant, B is the value of the magnetic field strength, and T is the temperature. The values of $T_0(= 4.56\ \mathrm{K})$ and $S_{\mathrm{eff}}(= 0.55)$ for $x = 0.2$ are determined empirically [16, 17], because of the antiferromagnetic Mn^{2+}–Mn^{2+} exchange interaction in the case of an Mn composition of $x > 0.05$. In thermal equilibrium, the $L2$ line originates from the transition $|-\frac{1}{2}\rangle \rightarrow |-\frac{3}{2}\rangle$ with σ^+ polarization.

Next, we examine the $L1$ line. A study of the A^0XBMP has been carried out in detail [14]. In non-magnetic CdTe, the deep acceptor impurities have been determined to be Ag and Cu, and the shallow acceptor impurities to be Li and Na [18, 19]. The $L1$ line is attributed to the exchange interactions between two Γ_8 holes with an angular momentum of $J_{\mathrm{h}} = \frac{3}{2}$ and one

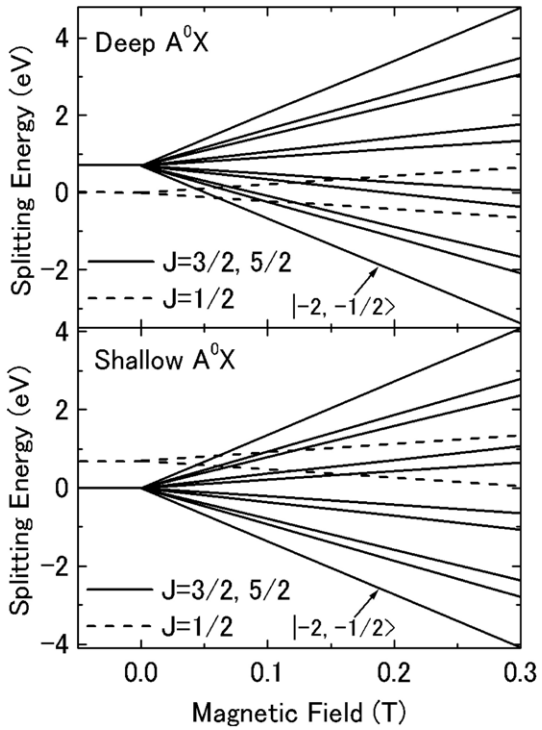

Figure 5. The Zeeman splitting for the deep A^0X and the shallow A^0X levels. After the energy-level crossings, the lowest energy level is $|-2, -\frac{1}{2}\rangle$.

Γ_6 electron with $J_e = \frac{1}{2}$. Due to the constraint of the antisymmetric combination in the j–j coupling scheme, the two Γ_8 holes form states of $J_{jj} = 0$ and $J_{jj} = 2$ [20]. Consequently, with the additional coupling to one electron with $J_e = \frac{1}{2}$, the lowest A^0X level for the deep acceptor is $J = \frac{1}{2}$, whereas those for the shallow acceptor are $J = \frac{3}{2}$ and $J = \frac{5}{2}$ [20–22]. The Zeeman splitting energy is rather large compared to the sub-meV energy separation between $J_{jj} = 0$ and 2 in an applied magnetic field, as shown in figure 5. Therefore, for both deep and shallow A^0X, the lowest level is $|-2, -\frac{1}{2}\rangle$, where $|m_{J_{jj}}, m_e\rangle$ is the A^0X state derived from two holes coupling $m_{J_{jj}}$ with one electron state m_e. The final acceptor state of the transition A^0 is the neutral acceptor state $J = \frac{3}{2}$. As a result, the lowest transition energy E_{tran} for the $L1$ line is $|-2, -\frac{1}{2}\rangle \rightarrow |-\frac{3}{2}\rangle$ with σ^- polarization, which is analogous to the procedure for the calculation for the $L2$ line. Because the energy level is formed on the basis of the hole energy in the A^0 state, the quantity $N_0\beta$ should be taken as being positive for both the hole in the A^0 level and the holes in the A^0X level; this is different from the assumption of a negative value of $N_0\beta$ for the electron in the valence band. The quantities of the exchange integral of a bound hole in both the deep and shallow A^0 should be reduced from 0.88 eV, whereas in the A^0X the exchange integral can be 0.88 eV, which is the same as that in a free hole because the Bohr radius of holes in A^0X is greatly expanded in space. With the hydrogen model, the wavefunction of the hole in A^0X is three times larger than that in A^0 [14, 23]. For a bound hole in the shallow A^0, we consider a known quantity of $N_0\beta = 0.65$ eV [14, 21], which results from the heavy and light hole mixing in the A^0 bound state [22]. The value of $N_0\beta$ for a bound hole in the deep A^0 is not yet known.

Figure 4 shows a comparison of the luminescence peak positions between the experimental results and the calculated results. In the previous calculations, the localization energy due to the APF and MP effects were not taken into account. Therefore, a constant APF localization energy should be considered over the entire value of the magnetic field, because the APF is modified very slightly by the external magnetic field. The MP effect is also considered only at a low magnetic field strength, because it vanishes under strong magnetic fields. At a high magnetic field strength, the energy difference between the reflectivity ($\diamond$) and the σ^+ luminescence peak ($\triangledown$) in figure 4 corresponds to the localization energy due to the APF. By overlapping the calculation results for the $L2$ line (broken line) and the σ^+ luminescence peak position ($\triangledown$) at a high magnetic field strength, the APF localization energy can be deduced to be 11 meV. This value is constant and independent of the applied magnetic field. The localization energy due to the MP is calculated to be 15 meV by subtracting (a) 11 meV from the total binding energy (a)+(b) at zero magnetic field strength. The MP localization energy of 15 meV is consistent with the selective excitation measurement [10]. Therefore, the higher-energy component of the photoluminescence spectra is attributed to EMP ($L2$, σ^+).

With regard to the $L1$ line, if the shallow acceptor participates, the calculation is performed with $N_0\beta = 0.65$ eV for holes in A^0. However, the theoretical computation yields much higher values for the photoluminescence peak energies compared to the experimental results. Therefore, the quantity $N_0\beta$ of a bound hole in the A^0 state should be smaller than 0.65 eV. Because a hole in the deep A^0 state is bound much more strongly than that in the shallow A^0 state, the exchange integral $N_0\beta$ of the deep A^0 state is quenched to a greater extended than that of the shallow A^0 state. Therefore, the $L1$ line is attributed to the deep acceptor. The solid line and open circles ($\bigcirc$) in figure 4 show a comparison between the experimental and theoretical results by adopting $N_0\beta = 0.35$ eV for a bound hole in the deep A^0. A good agreement is found for the σ^- photoluminescence at low magnetic field strength. Here, the A^0X binding energy without the MP effect is taken to be 7 meV [9]. Because the Bohr radius of the bound hole in A^0 is reported to be 8.5 Å [24] or 12 Å [14, 25] in the $Cd_{1-x}Mn_xTe$ bulk crystal, the binding energy may be large enough for the value $N_0\beta = 0.35$ eV to become possible. Therefore, the lower-energy component of the photoluminescence spectra should be attributed to A^0XBMP ($L1$, σ^-).

From the previous consideration, the double components of the time-evolution photoluminescence spectra (figure 2) should be attributed to the EMP and A^0XBMP. However, both components are hardly identified, because their energy difference is very small at zero magnetic field strength.

The modification of the thermal average value $\langle S_z \rangle$ due to the spin-diffusion bottleneck effect [13, 24] is not taken into account, because Mn^{2+}–Mn^{2+} spins are polarized by the MP effect within the lifetime of BMP in A^0XBMP [14]. It is important to note the dependence of the $L1$ line on the magnetic field. The $L1$ line reportedly disappears with a sufficiently strong external magnetic field [13, 14, 26]. This is attributed to the ionization of the A^0X state. Alternately, as shown in figure 3, the $L1$ line suddenly weakens with an applied magnetic field, but it persists and maintains a constant intensity. This response suggests that there is no direct relation between the $L1$ line and the $L2$ line. The constant intensity of the $L1$ line may be caused by the saturation of the excited A^0X states. As for the $L2$ line, the intensity increases by a factor of three with a strong magnetic field. This abrupt increase in the intensity may be ascribed to the directional dipole radiation in the Faraday configuration.

Finally, it is worth mentioning the photoluminescence experiment in the Voigt geometry. It has been reported that, in the case of the Voigt configuration, only the $L1$ line can be observed, whereas both the $L1$ and $L2$ lines appear in the Faraday configuration of $Cd_{0.9}Mn_{0.1}Te$ [13]. However, different experimental results, the appearance of the $L2$ line in both the Faraday and

Voigt configurations, have also been reported in $Cd_{0.88}Mn_{0.12}Te$ [12]. The experimental results obtained herein agree with the latter case.

4. Conclusion

The photoluminescence spectra of a single crystal of $Cd_{0.8}Mn_{0.2}Te$ were investigated as a function of time, magnetic field strength, and circular polarization. From a line-shape analysis of the photoluminescence spectra, it was found that the photoluminescence peak under band-to-band excitation is composed of two components. The higher-energy component (σ^+ polarization) is ascribed to the EMP, and the lower-energy component (σ^- polarization) is ascribed to deep A^0XBMP recombination. These results were obtained by accounting for the giant Zeeman splitting of the localized exciton and the exciton bound strongly to an acceptor. For EMP, the localization energy due to the MP effect and the APF were evaluated as 15 and 11 meV, respectively. Therefore, in this material the contribution of both effects of the exciton localization are comparable in energy. The exchange integral $N_0\beta$ of A^0XBMP has also been considered. By a theoretical analysis of the luminescence peak position at various magnetic field strengths, the value of $N_0\beta = 0.35$ eV for a bound hole in the deep acceptor, which is much less than that of the shallow acceptor, has been deduced. With an applied magnetic field, the constant intensity of the $L1$ line is caused by the saturation of the excited A^0X states. The enhancement of the intensity of the $L2$ line is due to the directional dipole radiation from EMP in the Faraday configuration. It is concluded that the above interpretations entirely explain the complexity of the edge-luminescence in $Cd_{0.8}Mn_{0.2}Te$.

Acknowledgments

T Okada sincerely thanks C Gourdon and P Lavallard in Groupe de Physique des Solides, Université Paris 6 et 7, CNRS UMR for fruitful discussions.

References

[1] Furdyna J K 1988 *J. Appl. Phys.* **64** R29
[2] Gaj J A, Byszewski P, Cieplak M Z, Fishman G, Gatazka R R, Ginter J, Nawrocki M, The Khoi N, Planel R, Ranvaud R and Twardowski A 1979 *Proc. XIV Int. Conf. Phys. Semicond.* (*Inst. Phys. Conf. Ser.* No. 43) p 1113
[3] Gaj J A, Galazka R R and Nawrocki M 1978 *Solid State Commun.* **25** 193
[4] Krenn H, Kaltenegger K, Dietl T, Spalek J and Bauer G 1989 *Phys. Rev.* B **39** 10918
[5] Kasuya T, Yanase A and Takeda T 1970 *Solid State Commun.* **8** 1543
[6] Oestreich M, Hübner J, Hägele D, Klar P J, Heimbrodt W, Rühle W W, Ashenford D E and Lunn B 1999 *Appl. Phys. Lett.* **74** 1251
[7] Schmidt G and Molenkamp L W 2001 *J. Appl. Phys.* **89** 7443
[8] Takeyama S, Adachi S, Takagi Y and Aguekian V F 1995 *Phys. Rev.* B **52** 1444
[9] Okada T and Itoh T 2002 *Proc. 26th Int. Conf. on Physics of Semiconductors (Edinburgh)* p H240
[10] Itoh T and Komatsu E 1987 *J. Lumin.* **38** 266
[11] Galazka R R, Nagata S and Keesom P H 1980 *Phys. Rev.* B **22** 3344
[12] Takeyama S, Adachi S, Takagi Y and Aguekian V F 1993 *Japan. J. Appl. Phys.* **32** (Suppl.) 425
[13] Heiman D, Becla P, Kershaw R, Ridgley D, Dwight K, Wold A and Galazka R R 1986 *Phys. Rev.* B **34** 3961
[14] Golnik A, Ginter J and Gaj J A 1983 *J. Phys. C: Solid State Phys.* **16** 6073
[15] Gaj J A, Planel R and Fishman G 1979 *Solid State Commun.* **29** 435
[16] Gaj J A, Grieshaber W, Bodin-Deshayes C, Cibert J, Feuillet G, Merle d'Aubigné Y and Wasiela A 1994 *Phys. Rev.* B **50** 5512
[17] Grieshaber W, Haury A, Cibert J, Merle d'Aubigné Y, Wasiela A and Gaj J A 1996 *Phys. Rev.* B **53** 4891
[18] Molva E and Dang L S 1983 *Phys. Rev.* B **27** 6222

[19] Molva E and Dang L S 1985 *Phys. Rev.* B **32** 1156
[20] Dean P J and Herbert D C 1979 *Excitons* (*Springer Topics in Current Physics* vol 14) ed K Cho (Berlin: Springer) chapter 3, p 55
[21] Bhattacharjee A K, Planel R and Bonoit à la Guillaume C 1985 *Proc. 17th Int. Conf. on the Physics of Semiconductors (San Francisco, 1984)* ed J D Chadi and W A Harrison (New York: Springer) p 1431
[22] Mycielski J and Rigaux C 1983 *J. Physique* **44** 1041
[23] Pan D S, Smith D L and McGill T C 1976 *Solid State Commun.* **18** 1557
[24] Heiman D, Warnock J, Wolff P A, Kershaw R, Ridgley D, Dwight K and Wold A 1984 *Solid State Commun.* **52** 909
[25] Golnik A, Gaj J A, Nawrocki M, Planel R and Benoit à la Guillaume C 1980 *J. Phys. Soc. Japan* A **49** (Suppl.) 819
[26] Planel R, Gaj J and Benoit a la Guillaume C 1980 *J. Physique Coll.* **41** (Suppl.) C5 39